Hydrogenolysis and β–elimination mechanisms for C S bond scission of dibenzothiophene on CoMoS edge sites

Alexandre Dumon, Amit Sahu, Pascal Raybaud

Hydrogenolysis and β–elimination mechanisms for C-S bond scission of dibenzothiophene on CoMoS edge sites

Alexandre S. Dumon[1], Amit Sahu[1,2], Pascal Raybaud[1,2,*]

[1] IFP Energies nouvelles, Direction Catalyse et Séparation, Rond-Point de l'Échangeur de Solaize, BP 3, 69360 Solaize, France.

[2] Univ Lyon, ENS de Lyon, CNRS, Université Claude Bernard Lyon 1, Laboratoire de Chimie UMR 5182, F-69342 Lyon, France

Emails: alexandre.s.dumon@gmail.com ; amit.sahu@ifpen.fr ; pascal.raybaud@ifpen.fr,

* Corresponding author: Pascal Raybaud, email : pascal.raybaud@ifpen.fr

ABSTRACT

Unraveling the mechanisms of hydrodesulfurization (HDS) of dibenzothiophene (DBT) and the corresponding active sites represents a scientific challenge to improve the intrinsic performances of Co-promoted MoS_2 (CoMoS) catalysts. By using density functional theory calculations, we compare two historical mechanisms for the C-S bond scission of DBT (direct desulfurization) : direct hydrogenolysis of DBT and β−elimination of α,β−dihydro-diobenzothiophene (α,β−DHDBT) on four relevant sites of the two CoMoS M- and S-edges. On the Co promoted M-edge, the α,β−DHDBT is formed through dihydrogenation which is kinetically competing with hydrogenolysis (both exhibiting activation free energies, $\Delta G^{\ddagger}$, smaller than +1.24 eV). On the S-edge, both dihydrogenation and hydrogenolysis exhibit higher $\Delta G^{\ddagger}$ (> + 1.78 eV). Interestingly, on the S-edge, the β−elimination (E2 type) on the α,β−DHDBT is found to be kinetically competing ($\Delta G^{\ddagger}$=+1.14 eV). The elimination of H_β atom involves a S_2 dimer close to the S-vacancy site where DHDBT is adsorbed. Since this leaving H_β atom is distinct from the one added at dihydrogenation step, this may explain why direct desulfurization of 4,6-alkyl substituted DBT compounds is hampered according to the elimination mechanism. We finally discuss the possible synergy between the two edges of CoMoS for HDS of DBT.

Keywords : hydrodesulfurization, dibenzothiophene, hydrogenolysis, β−elimination, CoMoS, edge sites, density functional theory

1. Introduction

Due to the ever stronger environmental concerns, hydrotreatment and more particularly hydrodesulfurization (HDS) remain the unique catalytic processes able to reduce the sulfur contents in diesel and gasoline so that these fuels meet the 10 ppm regulations. In order to improve the eco-efficiency of these processes and optimize the use of metals, it is crucial to keep on developing improved HDS catalysts with higher intrinsic activity of the active phase. The active phase of HDS catalysts is made of Co or Ni promoted MoS_2 [1-3], and it was historically identified as a so-called "mixed CoMoS phase" [4, 5]. Since these earlier findings, many experimental [2, 6-10] and theoretical [10-13] investigations have provided an ever deeper atomistic description of the potentially active sites located on the edges of the Co(Ni)MoS nano-crystallites. Nevertheless, challenging questions remain about the mechanism of transformation of sulfur containing polycyclic aromatic molecules such as derivatives of dibenzothiophene (DBT) on these edge-sites.

According to numerous experimental studies, the HDS refractory sulfur compounds are alkyl-substituted DBT, and more specifically the 4,6-dimethyldibenzothiophene (4,6-DMDBT) [14-17]. It is therefore crucial to better understand the HDS mechanism of this family of compounds in order to provide more efficient catalysts to achieve deep hydrodesulfurization at a lower energy process cost. For many years, this question has been addressed extensively by using kinetic studies combing both experimentation and modeling [18-25]. It is now largely accepted that the HDS of the family of DBT molecules undergoes via two-possible pathways: the hydrogenating (HYD) pathway, leading to cyclohexylbenzene (CHB) type compounds, while the second one, the direct desulfurization pathway (DDS), leads to biphenyl (BP) type compounds (**Fig. 1**) [21, 22, 25]. The probability of these two main pathways depend on the type of the DBT

derivative and on the nature of the catalyst. For DBT, the HYD pathway is preferred on non-promoted MoS_2 active phase, while the DDS pathway is predominant on Co(Ni)MoS phases. For 4,6-DMDBT, the HYD pathway is preferred on MoS_2 and Co(Ni)MoS [25], and its overall desulfurization activity is significantly lower than DBT.

However, according to experimental kinetic studies the DDS pathway may follow two competing mechanisms (**Fig. 1**). The first and most direct one, called hydrogenolysis [26], assumes that the DDS pathway undergoes via two successive H additions. The first H addition occurs on the C_α position of DBT (carbon in position α to S atom, also numbered C_4 carbon in the chemical nomenclature) and leads to the C-S bond breaking with the formation of the 2-phenyl-thiophenolate intermediate. The second H addition on the S atom would lead to 2-phenyl-thiophenol or intermediates [21]. The second possible DDS pathway proposes the formation of an α,β−dihydro-dibenzothiophene (DHDBT) intermediate by two H addition on the C_α and C_β positions of DBT (**Fig. 1**) [24, 25, 27]. DHDBT would be the precursor for the C-S bond scission by concomitant β−elimination (E2 type). Moreover, this alternative mechanism also assumes that the DDS and HYD pathways share a common DHDBT intermediate, that undergoes either the β−elimination, or subsequent hydrogenation steps. This concept of a common intermediate present at the crossing roads of DDS and HYD was earlier proposed by Singhal et al. [22]. However, it must be underlined that no direct experimental evidence of the formation of either DHDBT or 2-phenyl-thiophenol has been provided so far.

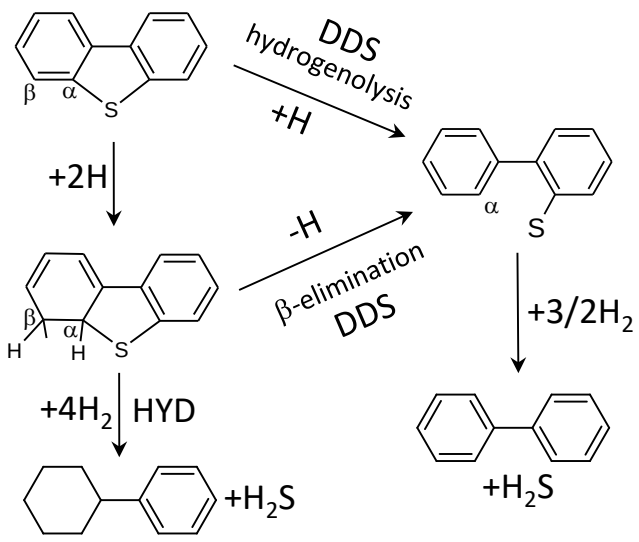

Fig. 1. Hydrodesulfurization of DBT through the DDS and HYD pathways involving either hydrogenolysis of DBT [28] or β−elimination of dihydrogenated DBT (DHDBT) [25]. Note: for sake of simplicity only the 2-phenyl-thiophenolate is represented but other intermediates such as 2-phenyl-thiophenol may form on the surface as discussed in the text.

At a molecular level, scanning tunneling microscopy (STM) combined with density functional theory (DFT) simulations have highlighted the various possible adsorption modes and energies of DBT derivatives on CoMoS supported on Au(111) surface [29-31]. These investigations reveal in particular how the underlying gold substrate may influence the spatial orientation of the DBT molecules adsorbed on the edge sites. DFT studies (including dispersion corrections) also showed that the adsorption energy and mode of 4,6-DMDBT on NiMoS depend closely on the nature of edge sites: in particular, 4,6-DMDBT is adsorbed perpendicularly with its S-atom located in a bridging position between two Ni sites of the S-edge, whereas it is absorbed in a nearly flat position on the Ni site of the promoted M-edge [32]. Since it is often suggested that

the HYD and DDS pathways might be controlled by the adsorption mode (either flat or perpendicular respectively) [27, 33], distinct activities are expected for the two edges. A similar proposal has been made by means of DFT simulation (without dispersion corrections) of DBT adsorption on non-promoted MoS_2 [34]. However, as the present work will illustrate, the link between the adsorption mode of DBT and the HYD/DDS pathways is not straightforward. Regarding the mechanistic aspects, Weber and van Veen investigated by DFT (without dispersion corrections) the hydrogenolysis mechanism of DBT on the Ni promoted M-edge site of a single NiMoS cluster [35], and showed that the first C-S bond breaking involves an activation energy of 1.37 eV. Surprisingly, this event is reported to occur during the DBT adsorption step on Ni site through a simultaneous H transfer from the same Ni site to the C_α atom of DBT. The possible formation of 2-phenyl-thiophenolate and 2-phenyl-thiophenol is also invoked in this study. By means of periodic DFT (without dispersion corrections), Paul et al. investigated the hydrogenolysis of DBT on the promoted S-edge of a CoMoS catalyst and found that the activation energy for the first S-C bond scission is about 1 eV: in this case, the H atom is transferred from a neighboring –SH group to the C_α atom of DBT [36]. More recently, the periodic DFT calculations of Saric et al. showed that the thiolate intermediates (including 2-phenyl-thiophenolate and methyl substituted 2-phenyl-thiophenolate) are stabilized preferentially on coordinatively unsaturated sites (CUS) of a CoMoS catalyst (either corner or at the edge) with respect to brim sites [37]. In addition, by applying a simplified linear combination of atomic orbitals scheme, activation energies for the first S-C bond scission on CUS were estimated at 1.2 eV, according to a hydrogenolysis mechanism. The same study showed that the activation energy is significantly higher on the brim S-edge site (~1.8 eV), which is partly due to the lower stability of the thiolate intermediate. Lastly, Ding et al. reported rather exhaustive DFT

calculations (including dispersion corrections) of the hydrogenolysis mechanisms of DBT and 4,6-DMDBT on various edges of a large NiMoS cluster [38]. They reveal that on a mixed Ni-Mo site located on the M-edge, the C_α-S bond breaking during the hydrogenation involves a significant rotation of the phenyl group of DBT which is hindered in the case of 4,6-DMDBT. Hence, the activation energy increases from 1.40 eV for DBT to 1.74 eV for 4,6-DMDBT. Moreover, they reveal that their activation energies are greater on the Ni promoted S-edge (1.95 and 2.12 eV, respectively).

At this stage, none of the published theoretical studies have investigated if such DDS pathways can take place on the partially Co-promoted M-edge. Numerous studies preferentially assumed that DBT desulfurization occurs exclusively on Co sites located on the S-edge. However, the partial location of Co on the M-edge has also been shown to be stable in HDS conditions by some of us [11, 39-42]. Thus, it is one goal of the present DFT work to explore if hydrogenolysis of DBT can take place on the partially Co-promoted edge and to determine the corresponding activation energies.

Moreover, it is important to address the alternative DDS pathway involving the hydrogenation of the C_α and C_β atoms of DBT followed by the β–elimination with S-C bond scission [24, 25]. To the best of our knowledge, none of the current theoretical studies has investigated the mechanism with a first hydrogenation in C_β position instead of C_α which may activate the elimination pathway as earlier proposed by Mijoin et al. [24]. This less straightforward pathway seems to be overlooked by many published studies without idenfying transition states (TS) and quantifying energy barriers. Thus, this will be the second challenge of this work to identify if the β–elimination pathway can take place on CoMoS sites.

2. Computational methods

The total energies were calculated using Density Functional Theory (DFT) [43, 44] calculations and were performed using the Vienna Ab Initio Simulation Program (VASP) [45, 46]. Within the generalized gradient approximation, the Perdew Burke and Ernzerhof (PBE) functional was used for the calculation of the exchange-correlation energies and the potentials [47]. The electron-ion interactions were described using the Projector Augmented Wave method (PAW) [48]. The density-dependent dispersion correction (dDsC) scheme was applied for including van der Waals interactions [49, 50]. In line with Ref. [32], dispersion corrections contribute strongly to adsorption energies of DBT by about 50%. We also noticed that the relative energy levels of intermediates involved in the reaction pathway are less impacted by values up to 0.1 eV (those of transition states being the least impacted, smaller than 0.01 eV).

The plane-wave cut-off expansion was set at 500 eV. Spin-polarization was included in order to take the magnetic properties of the M-edge induced by the presence of Co into account [51]. A Monkhorst-Pack mesh of 3x3x1 K-points was used for the 3D Brillouin zone integration.

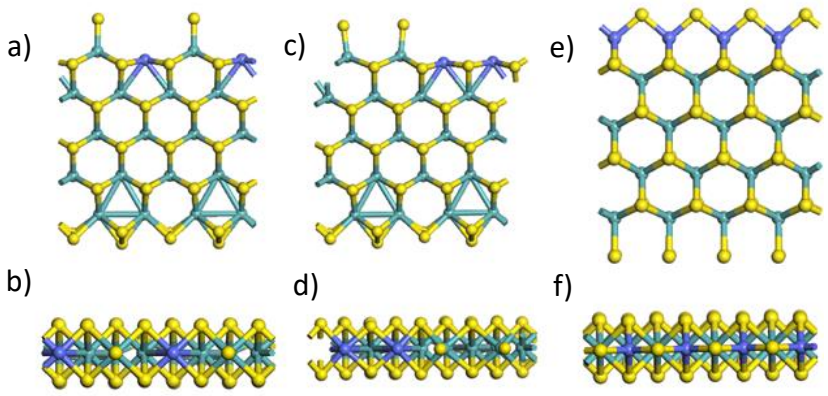

Fig. 2. Side and top views of the single slab stable in HDS conditions: M-edge with Co-Mo-Co-Mo site configuration (called "M-edge alternated" in the text) (a,b), with Co-Co-Mo-Mo site configuration (called "M-edge paired") (c,d) and of the reference S-edge with only cobalt sites (e,f). Color legend: blue balls: cobalt, green balls: molybdenum, yellow balls: sulfur.

In the same spirit as our previous DFT studies [39, 52], each edge was modeled by using five Mo layers, the top one being completed with the corresponding number of Co atoms represented in **Fig. 2** for the three edges stable in HDS conditions: the so-called M-edge and S-edge with Co atoms are substituting some of the Mo atoms on both edges. While the most stable S-edge is completely saturated by Co sites, the M-edge is partially promoted, presenting either Mo or Co sites: a configuration with …-Mo-Co-Mo-Co-… (called M-edge alternated) and a second one with …-Mo-Mo-Co-Co-… (called M-edge paired). Adsorption and reaction processes were performed on the top layer of the edges. While the bottom three layers were kept fixed in bulk positions during optimizations, the top two were relaxed.

The geometries were regarded as converged when the forces were smaller than 0.02 eV/Å. Transition states (TS) were determined using a combination of a path extrapolator [53] with the nudged elastic band (NEB), climbing image – NEB [54, 55], and dimer methods [56]. The status

of the TS was confirmed by the presence of a single imaginary frequency associated to the corresponding reaction coordinate. In the specific case of the β−elimination mechanism (E2 type), which involves numerous bond breaking/formation events, we confirmed the minimum energy path connecting the reactant, TS and product by undertaking an Intrinsic Reaction Coordination (IRC) analysis [57, 58].

All frequencies were calculated within the harmonic approximation. Some TS (respectively intermediates) exhibit two (respectively one) imaginary frequency with absolute values smaller than 30 cm^{-1}. Very few spurious imaginary frequencies (when they exist) were assumed to correspond to residual translational or rotational modes and were removed together with the five smaller frequencies in order to evaluate the free energies of adsorbed species considered as immobile adsorbate [59]. Alternative approaches such as replacing the spurious imaginary frequency by a normal mode of positive value [59] showed minor impact on the reported thermodynamic trends. The Gibbs free energy, G, is expressed as a function of the enthalpy H and entropy S of the system:

$$G = H - TS \quad (1)$$

$$H = U_{elec} + U_{vib} + U_{trans} + U_{rot} + pV_m \quad (2)$$

$$S = S_{elec} + S_{vib} + S_{trans} + S_{rot} \quad (3)$$

where $U(S)_{elec}$, $U(S)_{vib}$, $U(S)_{trans}$, $U(S)_{rot}$ and V_m are respectively the electronic energy (entropy), vibrational energy (entropy) including "zero point energy", translational energy (entropy), rotational energy (entropy) and the molar volume. The molar volume term pV_m was considered for an ideal gas system and for condensed phase systems, H was assimilated to U. The electronic energy was obtained by DFT calculations, while other energy terms were

calculated from statistical thermodynamics based on the vibrational frequencies previously calculated.

3. Results and discussion

3.1 Adsorption configurations of DBT on 4 relevant edge sites

The most stable adsorption modes of DBT in presence of co-adsorbed H_2 on each edge is represented in **Fig. 3**, along with their corresponding adsorption energies (including H_2 adsorption) according to the following equation:

$$G_{ads} = G(edge + H_2 + DBT) - G(edge) - G(H_2) - G(DBT) \quad (4)$$

where $G(slab + H_2 + DBT)$, $G(edge)$, $G(H_2)$, and $G(DBT)$ respectively corresponds to the free energy of the given edge with adsorbed H_2 and DBT, of the corresponding bare edge, the H_2 and DBT molecules, respectively. The bare edges are given as references in **Fig. 1**. For the S-edge, the adsorption energies include the energy required to create the CUS: either through S-removal (**Fig. 3c**) or through S-diffusion (**Fig. 3d**), as discussed later.

Previous studies have shown that the H_2 dissociation on the three edges was weakly activated and endothermic [60, 61]. Considering DBT and H_2 adsorption, the resulting overall adsorption energies become exothermic due to the negative adsorption energy of DBT whatever the edge. However, when including entropic contributions, the free energies of adsorption become endergonic due to the significant loss of rotational and translational entropies of the DBT and H_2 molecules (**Fig. 3**) as it has already been reported in previous theoretical studies for similar sulfur or nitrogen-containing organic molecules [32, 37].

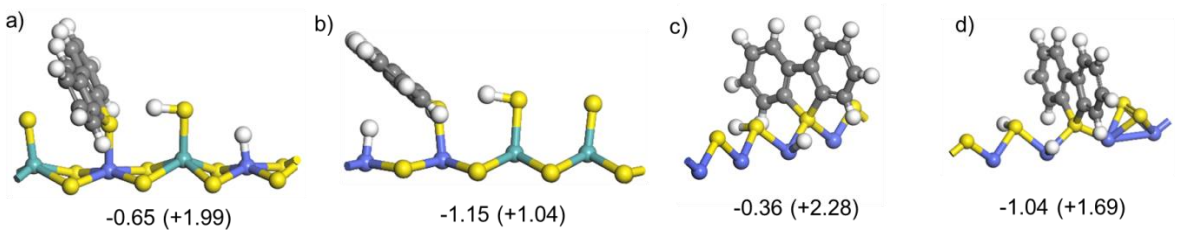

Fig. 3. DBT+H_2 most stable co-adsorption on M-edge alternated (a), M-edge paired (b), S-edge with S-removal (c), and S-edge with S-diffusion (d). The overall adsorption energies and free energies (in parenthesis) of DBT+H_2 are given in eV. These energies include the S-removal and S-diffusion energies for the S-edge. Color legend: blue balls: cobalt, green balls: molybdenum, yellow balls: sulfur, dark grey balls: carbon, light grey : hydrogen.

On the M-edge alternated, the DBT adsorbs in a slightly tilted η_1-mode through its S atom on top of the Co-promoter site located between one edge S and one –SH species, while the H_2 dissociates and adsorbs on the neighboring sulfur atom and the remaining Co-promoter (**Fig. 3a**) The DBT is slightly tilted toward the non H bearing surface S atom, while the –SH group is directly pointing towards the DBT molecule which features the formation of a hydrogen bond with the aromatic rings. It must be noticed that the symmetric configuration where DBT molecule is tilted toward the –SH species is not favorable because of the too close proximity of the H atom. As for the M-edge alternated, on the M-edge paired, the H_2 molecule is dissociated on one surface –S atom and one Co site, leading to Mo-SH and Co-H species (**Fig. 3b**). On the M-edge paired, the DBT molecule is even more tilted, and becomes in close interaction with the Co-H group with the formation of a second H-bond. This H-bond explains why the adsorption energy is more exothermic (less endergonic) on the M-edge paired than on the M-edge alternated.

On the S-edge, we compared the adsorption and reaction of DBT on two different models. The first one includes one S-vacancy (CUS) created by S-removal upon H_2/H_2S exchange (**Fig. 3c** and **Fig. 4a**), often reported in the literature [36, 37]. The second one assumes that CUS is created by edge diffusion of one S-atom from one bridging position to the next one inducing the formation of a S_2 dimer (S-S bond length ~2.03 Å) in the vicinity of the S-vacancy (**Fig. 3d** and **Fig. 4b**). The energy cost to create the S-vacancy by S-removal upon H_2/H_2S exchange is +1.66 eV (ΔG=+1.85 eV), whereas the diffusion of one S atom is less energy demanding +0.97 eV (ΔG=+1.03 eV). The corresponding activation energy for the S-diffusion is +1.61 eV ($\Delta G^{\ddagger}$=+1.48 eV) which is also more favorable than the thermodynamic balance for S-removal. This edge state with the presence of a CUS associated to S_2 dimer should be considered as a transient metastable state which comes back to the thermodynamic stable state at the end of the catalytic cycle. For this, the last step will involve a S-removal step from the dimer species at a moderate energy cost of +0.48 eV (ΔG +0.19) as detailed in section 3.4. Hence, the diffusion of S-atom is a more plausible scenario to generate transient CUS at edge than direct S-removal.

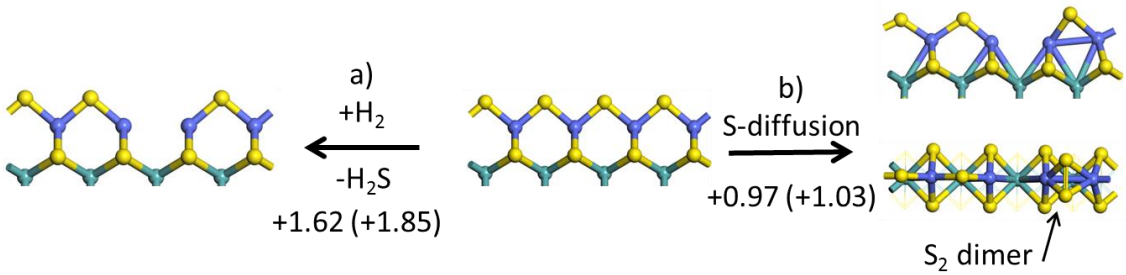

Fig. 4. Two possible processes creating two possible transient metastable states with one S-vacancy (CUS) from the most stable S-edge model: a) sulfur removal by H_2/H_2S exchange, b) sulfur edge-diffusion forming one S_2 dimer neighboring the vacancy. The reaction energies at 0K and free energies (in parenthesis) are given in eV.

For both S-edge models, the most favorable adsorption configuration of DBT is found in a bridging position between two Co atoms. DBT remains perpendicularly oriented to the edge and no close H-bond is formed. The DBT adsorption on the second S-edge model can be considered as a collaborative process: the DBT molecule approaching the surface, pushes one edge S-atom toward another neighboring S, creating a vacancy and the S_2 dimer. The H_2 molecule is dissociatively adsorbed on one surface –S atom and one Co site. If one include the energy cost for S-diffusion, the overall energy variation for the S-diffusion and adsorption of DBT and H_2 is (ΔE=-1.04 eV, ΔG=+1.69 eV) which is more favorable than on the S-edge after S-removal (ΔE=-0.36 eV, ΔG=+2.28 eV).

These four starting configurations will serve for investigating the DBT hydrodesulfurization pathways in the forthcoming sections. In the main text, we will report and discuss for sake of clarity the Gibbs free energy profiles obtained on the alternated M-edge and of the S-edge after S-diffusion only. The results for the two other cases are reported in supplementary information where all energy profiles are given and discussed.

3.2 Direct hydrogenolysis of DBT on the alternated M-edge

Following the DBT+H_2 adsorption described in the previous section, the first step is the monohydrogenation of C_α by the neighboring –SH species which exhibits an activation free energy of +1.16 eV. The corresponding TS A(1-2)‡ involves the H atom significantly elongated from the –SH group and the C_α atom that bends outward the cycle closer to the transfered H atom (**Fig. 5)**. TS A(1-2)‡ can be characterized as a late-TS, resembling the α-monohydrogenated

DBT intermediate A(2), with an activation energy closer to the free energy variation of this elementary step (+1.02 eV).

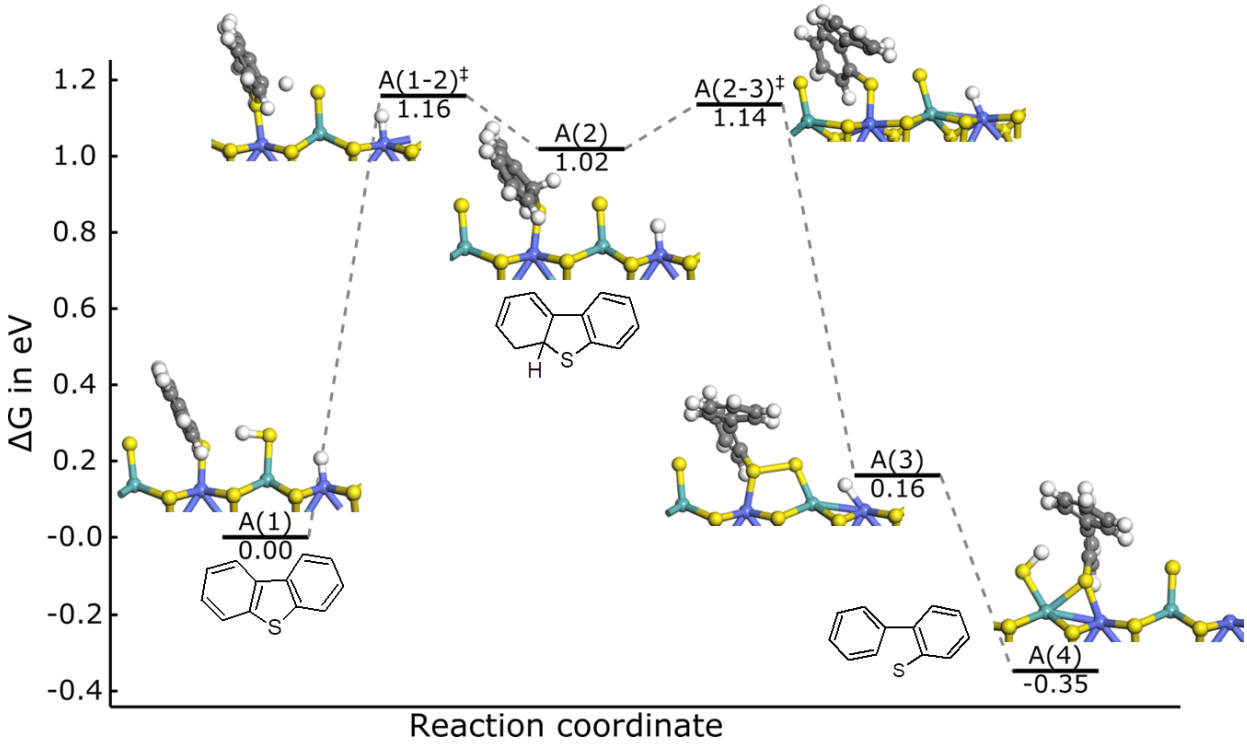

Fig. 5. Free energy profile of the hydrogenolysis of the first C-S bond scission of DBT to biphenyl (BP) on the M-edge alternated involving the 2-phenyl-thiophenolate intermediate.

Once the C_α-H bond is formed, a weakly activated rotation of the phenyl group (TS A(2-3)‡ at +0.12 eV) leads to the first C-S bond breaking and the formation a 2-phenyl-thiophenolate intermediate A(3) stabilized by a S-S bond (2.27Å) formed between the S atom of the thiophenolate intermediate and the neighboring Mo-S species. The rotation of the phenyl group occurs in the direction given by the position of H_α atom (the same will occur on the S-edge).

The overall free energy variation for the C-S bond scission from adsorbed DBT+H_2 to thiophenolate is slightly endergonic (+0.16 eV). It becomes exergonic (-0.35 eV) after diffusion of H from a Co site to the Mo-S group and thiophenolate migration in a bridging Co-Mo position (A(4)).

According to the proposal made in Ref. [37], the stabilization level of 2-phenyl-thiophenolate might be a descriptor of the hydrogenolysis mechanism. However, it must be noticed that the two TS, A(1-2)‡ and A(2-3)‡, as well as the α-monohydrogenated DBT intermediate, A(2), are located at significantly higher energies (~ +1 eV) than thiophenolate. This may be an indication that the thiophenolate stabilization is one necessary condition but probably not the sole descriptor for featuring if hydrogenolysis is kinetically possible or not. Analyzing the calculated reaction and activation energies for DBT and alkyl-DBT HDS on NiMoS sites reported by Ding et al., showed that there is no direct correlation between the thiophenolate energy and the activation energy of hydrogenolysis for the various edge and corner sites [38]. Actually, the energy level of the TS is linked to various contributions: the energy level of the α-monohydrogenated DBT intermediate, the steric hindrance of the rotational movement of the phenyl group during the C-S bond scission and the optimal position of the –SH groups involved in the H-transfer (see also further discussion). Hence, these three kinetic effects cannot be deciphered by a single descriptor based on the stability of the 2-phenyl-thiophenolate intermediate. In addition, depending on the DFT study, the existence of the α-monohydrogenated DBT intermediate as an intermediate is not always reported [36, 38] which is explained by its relative weak stability with respect to TS A(1-2)‡ and A(2-3)‡. The potential energy surface in the vicinity of TS A(1-2)‡, A(2) and A(2-3)‡ will thus intimately depend on the local nature of the edge site (see also later for the S-edge).

From 2-phenyl-thiophenolate A(4), two possible pathways can be considered. The first one involves the formation of a 2-phenyl-thiophenol intermediate leading to the second C-S bond scission, as described in detail in **Fig. S2**. The second one involves a direct C-S bond scission of 2-phenyl-thiophenolate. For that purpose, a second H_2 molecule adsorption which leads to the thiophenolate co-adsorbed with two neighboring Mo-SH groups (**Fig. 6**). From this configuration, the second C_α hydrogenation by one SH can proceed in a similar way as the first one and the TS A(5-6)‡ exhibits a similar free activation energy of +1.35 eV. This second C-S bond breaking step leads to a physisorbed biphenyl (BP). Similar activation energies are found for the thiophenol pathway (**Fig. S2**) and will be discussed later for the second C-S scission on the S-edge (section 3.4). These values remain compatible with previously calculated activation energies of hydrogenolysis of alkane thiols on MoS_2, CoMoS and NiMoS edges [62-64]. The fact that the activation energy of the second C_α-S bond scission is similar or even slightly higher than the first one seems to be counter-intuitive since the conjugaison of S-lone pair electrons with those of the aromatic rings is expected to limit the first C-S bond cleavage. However, our TS analysis reveals that another effect may influence the relative activation energies of the two C_α-S bond scission: the optimal position of the Mo-SH group to attack the C_α atom during H-transfer. As illustrated in **Fig. S8**, the imaginary frequency of the reaction mode corresponding to the H-transfer (leading either to hydrogenolysis or to hydrogenation as detailed latter) is mainly correlated to the SH bond length. This trend indicates that the position and accessibility of –SH group is a key parameter for the activation step. In the case of the second bond C-S cleavage, the reorientation of the phenyl ring in 2-phenylthiophenol which becomes parallel to the edge hinders the optimal position of the second C_α atom with respect to the neighboring Mo-SH

group. Hence, the C-S bond breaking of 2-phenylthiophenol might not be as easy as usually observed for model thiols or thiophenol molecules.

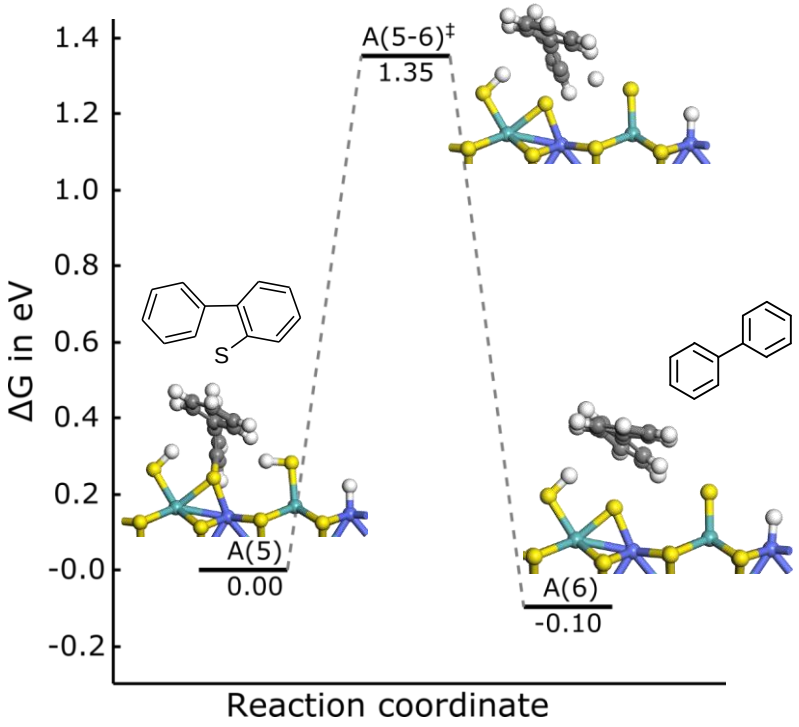

Fig. 6. Free energy profile of the second C-S bond scission on the M-edge alternated involving the 2-phenyl-thiophenolate and leading to biphenyl product.

After the BP molecule is desorbed, we reasonably assume that the remaining H atom reaches the S-H group, to form H_2S and desorb to recover the initial M-edge thermodynamically stable in typical HDS conditions (**Fig. S1**) [39]. The overall free energy variation for the BP+H_2S desorption is about +0.75 eV which is mainly due to the BP desorption energy involving mainly dispersion and H-bond interactions of BP on the edge.

According to the slightly different levels of theory of previous studies (cluster vs periodic systems, with or without dispersion corrections), the activation energies calculated for the two

C_α-S bond scissions within the present work are either as competitive or even more competitive than those reported previously for different edge sites such as M-edge and S-edge of NiMoS [35, 38] and S-edge of CoMoS [36, 37]. This implies that the partially Co-promoted edge, with alternated Co-Mo-Co-Mo sites, is a relevant active edge for the hydrogenolysis pathway of DBT compounds.

Considering now the promoted M-edge with paired cobalt atoms, we start from the most stable configuration of **Fig. 3b** for DBT+H_2 adsorbed. However, on this edge configuration, we did not identify any relevant TS leading to the α–monohydrogenation from the –SH group which may be explained by the fact that the position of the hydrogenating –SH species is too far from the aromatic rings of DBT. Indeed, **Figs. 3b** and **3a** reveal that the tilting angles of DBT are not the same for the promoted M-edge paired and unpaired, which impact the accessibility of –SH. By contrast, the Co-H group which is located in closer interaction with the aromatic will be involved in these hydrogenation steps. We tried to hydrogenate in α position from the Co-H but the monohydrogenated intermediate is not stable and the H atom relaxes back to the Co site, while the S-C bond cleavage was not found possible due to steric hindrance during the rotational movement of the phenyl group. The alternative possibility of the hydrogenation in β position will be discussed in the forthcoming sections.

3.3 Dihydrogenation pathways leading to dihydrogenated DBT (DHDBT)

3.3.1 Case of the M-edge sites

As explained in the Introduction, we investigate in this section the alternative DDS pathway as proposed in the literature [24, 25], which consists in the preliminary formation of the DHDBT intermediate with C_α and C_β hydrogenation occurring on the same phenyl ring. After the first monohydrogenation C_α-H step, the second monohydrogenation of the molecule may occur by transferring the second H atom to C_β. However, our attempts to achieve this second hydrogen transfer either failed or involved energy costs greater than the modest activation energy (+0.12 eV) found for the first C-S bond breaking during the rotation of the phenyl ring of α-monohydrogenated DBT (as described before). Thus, once α-monohydrogenated DBT is formed by C_α hydrogenation, its further C_β hydrogenation seems to be unfavored with respect to the easier C_α-S bond breaking. To some extent, this result may also explain why many theoretical studies did not explore this pathway so far and preferentially followed the hydrogenolysis step. Alternatively, the hydrogenation pathway must be initiated by the hydrogenation of DBT in the C_β position as initially suggested by Mijoin et al. [24]. Starting from DBT+H_2 adsorption, the free energy profile corresponding to the two C_β followed by C_α monohydrogenation steps is reported in **Fig. 7**.

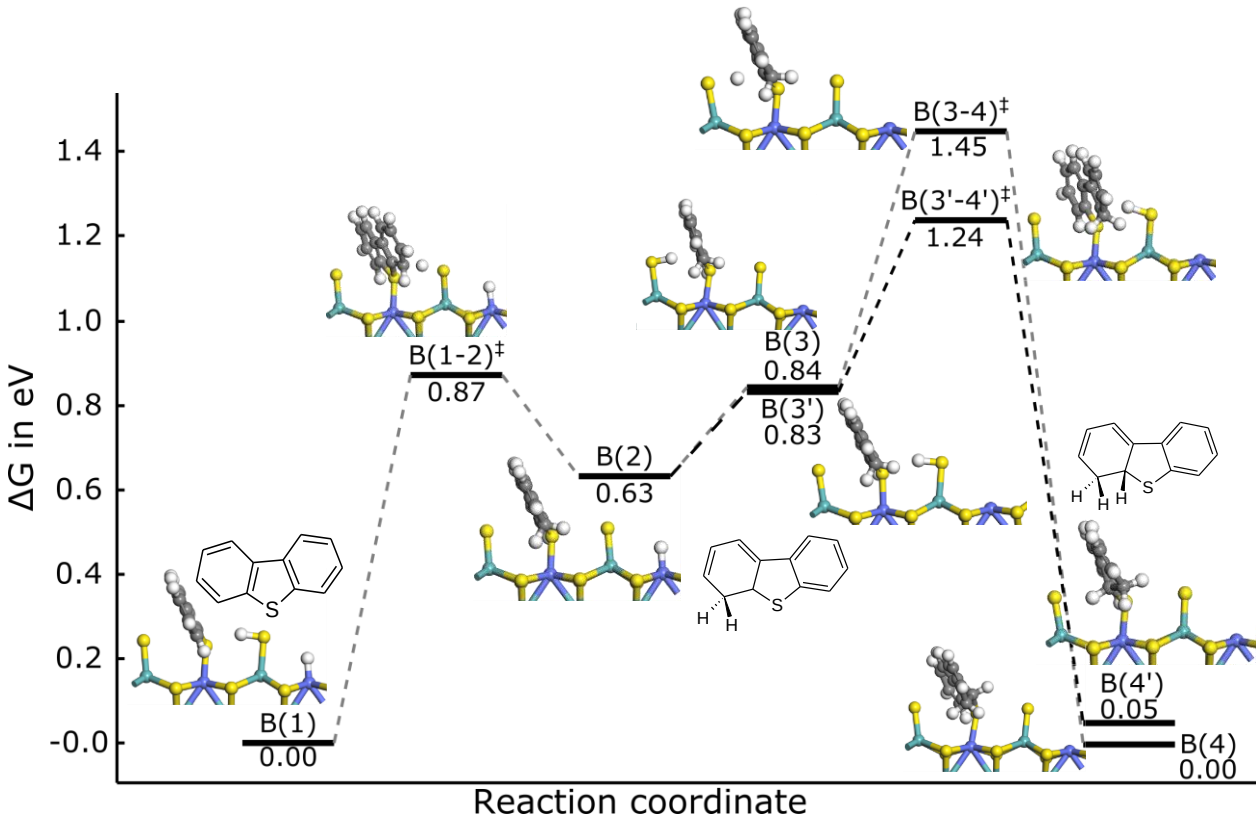

Fig. 7. Free energy profile of the C_β followed by C_α hydrogenation steps of DBT leading to the β,α-dihydrogenated DHDBT intermediate. B(3-4)‡ corresponds to anti-pathway, B(3'-4')‡ to syn-pathway.

The activation free energy of the first monohydrogenation in C_β (through H transfer coming from a -SH group) is rather modest (+0.87 eV for B(1-2)‡) and is significantly lower than the one found for the previous hydrogenation at C_α. This value is also lower than any previous activation energy reported in the literature for the hydrogenolysis pathway so far; often greater than 1.3 eV [35, 37, 38], except results in [36] where dispersion corrections were not considered. The β-monohydrogenated DBT intermediate B(2) is thermodynamically more stable than α-monohydrogenated DBT A(2) by about -0.39 eV which is coherent with the kinetic trend,

considering the late-TS character of both B(1-2)‡. The preferential hydrogenation in β than in α can be explained by the destabilization of α–hydrogenated intermediate or related TS, induced by the loss of conjugation involving the S lone pair electrons.

After this first monohydrogenation, the remaining H atom can diffuse to two possible Mo-S sites from which the second monohydrogenation in α position may occur through anti-B(3-4)‡ or syn-B(3'-4')‡ transfer and lead to two similar DHDBT conformers B(4) or B(4'), respectively in **Fig. 7**. In both cases, the reaction energies are exergonic (of -0.78 and -0.84 eV respectively), while both activation energies are pretty mild (+0.62 eV and +0.41 eV). Thus, the attack in α is stereospecific due to the different relative position of the tilted monohydrogenated-DBT and Mo-SH group. As observed for the hydrogenolysis mechanism, the frequencies of the reaction modes are strongly governed by the –SH stretching depending on the relative positions of the –SH groups and targeted carbons, C_α or C_β (**Fig. S8**). Considering the first two hydrogenation steps, and applying an energetic span concept [65], the overall activation free energy corresponding to the formation of the dihydrogenated DHDBT intermediate is about +1.24 eV, which makes this pathway as competitive as other hydrogenation steps simulated either in the present study or in previously published works [35-38].

Although the existence of the DHDBT intermediate has been questioned in the experimental literature [21, 66], the present results reveal that it cannot be ruled out from a thermodynamic and kinetic point of view. From a thermodynamic point of view, the free energy level of DHDBT is also acceptable since it is only +0.49 eV higher than the iso-stoichiometric 2-phenyl-thiophenol intermediate which may be formed during hydrogenolysis.

Considering the promoted M-edge with paired cobalt atoms, the mechanism and energy profile reported in **Fig. S4** show that both hydrogenation steps involve preferentially H transfer from the Co-H site (and not from Mo-SH) with a moderate overall activation energy (+1.29 eV). Since it was not possible to identify a hydrogenolysis pathway on this type of edge (as mentionned in the previous section), we think that the dihydrogenation pathway occurs with a non negligible probability, knowing that the M-edge with such paired Co sites may co-exist according to previous DFT [39] and experimental studies [67].

3.3.2 Reaction on the S-edge sites

Since the dihydrogenation steps occur in a similar way on both types of S-edge sites illustrated in **Figs. 3c** and **3d**, we focus in the main text on the one corresponding to the S-vacancy obtained by S-diffusion (**Fig. 4b**) which is thermodynamically and kinetically favored with respect to the one where the S-vacancy is obtained by S-removal (**Fig. 4a**).

From the H_2 molecule dissociated on one S-atom and on one Co-atom, the Co-H species preferentially hydrogenates the two C atoms in α and β positions because of the unfavored orientation and distances of H from –SH group and the two C atoms : ~3.5 Å from the S-H to the α and β positions, compared to ~3 Å from the Co-H to the α and β positions. So, the first C_α monohydrogenation occurs through the Co-H species with an activation free energy of +1.61 eV ($C(1\text{-}2)^{\ddagger}$) and the second H also transferred through Co-H with an overall activation free energy +0.77 eV (including H diffusion step from –SH to Co-H and then $C(3\text{-}4)^{\ddagger}$). If we apply the energetic span concept for the dihydrogenation steps, we identify an overall activation free energy of +1.78 eV, which is higher than all activation free energies found on the M-edge. Since

a similar trend is reported for the S-edge site with S-vacancy after S-removal (**Fig. S6**), this indicates that the S-edge is less active for hydrogenation steps than M-edge.

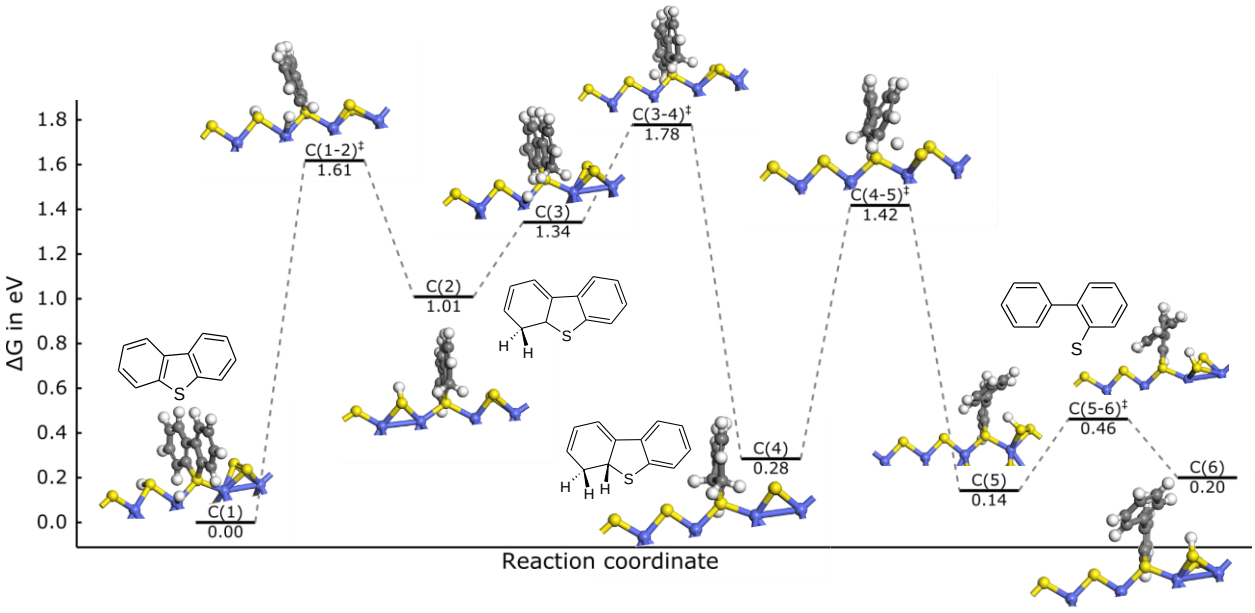

Fig. 8. Free energy profile of the DDS of DBT through β–dehydrogenation mechanism on the S-edge with preliminary S-diffusion leading to the formation of one S-vacancy and one neighboring S_2 dimer.

3.4 Dehydrogenation pathways and S-C bond scission of DHDBT according to E_2 mechanism

Interestingly, on the promoted S-edge with S-vacancy and neighboring S_2 dimer, the β elimination with simultaneous C-S bond breaking can proceed with a reasonable activation free energy of +1.14 eV for TS C(4-5)‡ in **Fig. 8**. This mechanism involves three chemical events as described in the insets of **Fig. 9**: transfer of H in β position to the edge S atom, C-S bond scission, phenyl ring rotation and weakening of the neighboring S_2 dimer.

In order to confirm the validity of this complex mechanism and more particularly the connection between the reactant C(4), TS C(4-5)‡, and product C(4), we undertook a dedicated IRC analysis. This analysis clearly shows the key role of the S_2 dimer which captures the H_β-atom transferred from the C_β atom of DHDBT C(4) with the reactive mode frequency of 925 cm^{-1}. Interestingly, this mode also fits the correlation between frequency and SH bond length previously discussed for the hydrogenation steps (**Fig. S8**). In the starting conformation of DHDBT, the H_β involved in the transfer is located in anti-position to H_α which is the most favorable position to reach one S of the dimer.

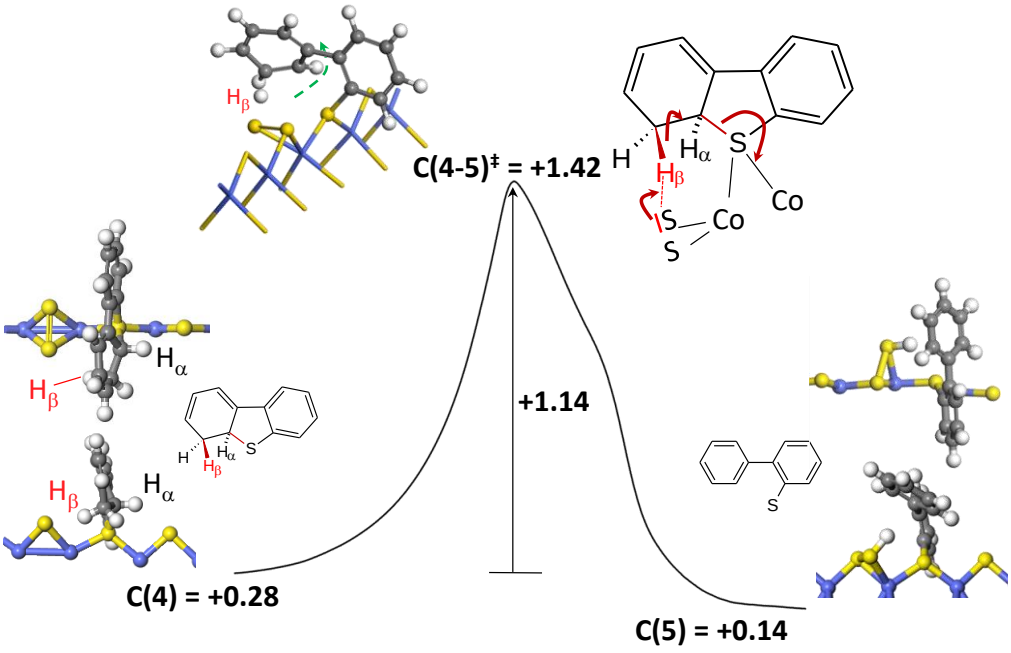

Fig. 9. Intrinsic Reaction Coordinate (IRC) path connecting reactant, TS and product of the β–elimination (E2) mechanism with S-C bond scission involving the S_2 dimer of the S-edge. The black line illustrates the energy evolution along the minimum energy path crossing the saddle point C(4-5)‡. The H_β atom involved in the transfer is written in red, while the H_α is written in black. The broken S-C bond is drawn in red. The green dashed arrow highlights the rotational movement of the phenyl group. The red arrows represent the formal electronic transfer involved. All energies are in eV.

At TS C(4-5)‡ the rotation of the phenyl group occurs simultaneously with the C_α-S bond scission. In the product, the S_2 dimer is not fully dissociated and an intermediate C(4) SSH species is formed. Hence, as earlier proposed by Bataille et al. [25], this mechanism is a true elimination of E2 type: the protonic H_β atom is captured by the S anionic base of the S_2 dimer, while the anionic S atom of DHDBT acts formally as the nucleofuge species stabilized by the Co cationic center and induced the C_α-S bond scission. The apparent leaving group is the phenyl group which rotates away from the S atom of DHDBT. The complete IRC path is presented on the movie provided in supplementary materials.

An important corollary is related to the stereochemistry of H_β atoms involved in the dehydrogenation and elimination mechanisms. In the same way as for the TS of hydrogenolysis, the rotation of the phenyl group occurs in a direction following the position of H_α atom. However, the leaving H_β atom is located in anti-position of both H_β and H_α atoms transferred during the dihydrogenation step. Hence, the H_β added during hydrogenation and the leaving one during elimination are not obligatory the same. This implies that for 4,6-alkyl substituted DBT compounds, the position of the H_β atom involved in elimination is occupied by an alkyl group. Hence, the DDS pathway through the elimination mechanism proposed here, will be hampered. The present analysis based on stereochemistry provides a refinement of the original explanation suggested by Bataille et al. to justify the lower reactivity of 4,6-DMDBT [25].

Interestingly, the role of S_2 dimer in the reactivity of unsupported MoS_2 phase has been previously discussed in the experimental work of Afanasiev [68]. Moreover, scanning tunneling microscopy (STM) combined with DFT calculations have shown that S_2 dimers exist in some sulfiding conditions on the Mo-edge of MoS_2 [69, 70]. We thus propose here that S_2 dimer could

be transiently formed through edge diffusion of S-atom described in section 3.1 in order to promote the reactivity of CoMoS edges. On the fully Ni promoted S-edge, Ding et al. [38] simulated the hydrogenolysis mechanism of DBT involving such S_2 dimers, stable in HDS conditions [11, 39]. Once H_2 molecule adsorbs dissociatively, the S_2 dimer dissociates into two –SH groups, one of which H is transferred to DBT [38].

To achieve a more consistent comparison for the CoMoS case, we simulate this similar hydrogenolysis mechanism of the first C-S cleavage involving H-transfer from one of the two neighboring –SH groups on the Co promoted S-edge (D(1) in **Fig. S8**). The free energy of activation for D(1-2)‡ is found at +1.83 eV which is close to value reported for NiMoS [38]. D(1-2)‡ leads to thiophenolate D(2) without formation of α–monohydrogenated DBT intermediate (contrasting with M-edge). In addition, the H-transfer to C_α from Co–H species (as previously explored for the C_β hydrogenation) also reveals that the direct C-S bond cleavage leads to thiophenolate with a similar free energy of activation of +1.85 eV (TS E(1-2)‡ in **Fig. S7**). In both cases, the rotation of the phenyl group is again driven by the incoming H_α atom. The fact that the activation energies for hydrogenolysis are higher on the S-edge than on the M-edge is correlated to the instability of the α–monohydrogenated DBT which is not found as stable intermediate on the S-edge. On the M-edge, the transient formation of the α–monohydrogenated DBT is a preliminary step to weaken the S-C_α chemical bond which is broken in a second step. By contrast, on the S-edge the S-C_α breakage occurs simultaneously to the H transfer which leads to a higher activation energies. More generally, this complete analysis confirms that the β–elimination mechanism is kinetically possible once the α,β–DHDBT is formed.

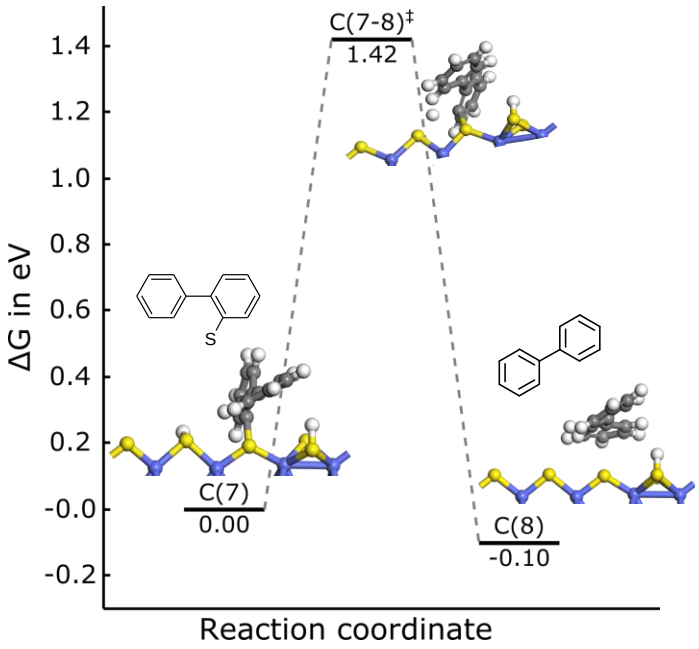

Fig. 10. Free energy profile of the second C-S bond scission on the S-edge with preliminary S-diffusion leading to the formation of one S-vacancy and one neighboring S_2 dimer.

The second C-S bond scission occurs through a direct hydrogenolysis mechanism involving an –SH species with an activation free energy of +1.42 eV (C(7-8)‡ in **Fig. 10**), and produces biphenyl (BP). This value is very similar to the one obtained on the M-edge. Again, the frequency of the reaction mode is closely related to the –SH bond stretching (**Fig. S8**). Contrasting with the M-edge, the activation energy of the second C-S bond scission is now smaller than the first C-S bond scission (either through hydrogenolysis or through a dihydrogenation-elimination mechanism) which is in line with the chemical intuition. Since the activation free energies of the second C-S bond scission are similar on M-edge and S-edge, this trend results from the different activation free energies of the first C-S bond scission on S-edge and M-edge which may have significant implications on the design of the CoMoS active phase.

Finally, to close the loop of the catalytic cycle and recover the thermodynamically most state of the S-edge, biphenyl desorbs and the excess S atom is removed upon H_2/H_2S exchange. The energy cost (ΔE=+0.48 eV and ΔG=+0.19 eV, see Fig. S5) for this last step is significantly more favorable than the scenario where S-vacancy is created on the most thermodynamically S-edge (Fig. 1) which justifies the S-diffusion process with S_2 dimer formation.

4. Conclusions and perspectives

By means of DFT calculations including dispersion corrections, we investigated the HDS mechanisms of DBT and determined the corresponding free energy profiles considering four relevant adsorption configurations of DBT on 4 relevant types of CoMoS active sites:

- M-edge with alternated Co-Mo-Co-Mo sites exhibiting Co sites and neighboring Mo-S sites
- M-edge with paired Co-Co-Mo-Mo sites exhibiting Co sites and neighboring Co and Mo-S sites
- S-edge with one S-removal exhibiting one S-vacancy on Co-site
- S-edge with S-diffusion leading to S-vacancy on Co-site and S_2 dimer

Depending on the nature of the edge, the hydrogenation steps involve either Mo–S and Mo–SH species, or Co-H species adsorbed in close vicinity of the DBT adsorption Co site. The most relevant free energy profiles are summarized in **Fig. 11**.

On the M-edge with alternated Co-Mo-Co-Mo sites, we identified two competing mechanisms for the direct hydrogenolysis of the C-S bonds of DBT involving either the 2-phenyl-

thiophenolate or the 2-phenyl-thiophenol intermediate. Both mechanisms are activated by the formation of the α–monohydrogenated intermediate through Mo-SH species. In the case of 2-phenyl-thiophenolate, the free energy of activation is +1.16 eV. The stabilization of the α–monohydrogenated intermediate (not observed on the S-edge) should be at the origin of this moderate activation energy for the S-C bond scission which occurs in two steps.

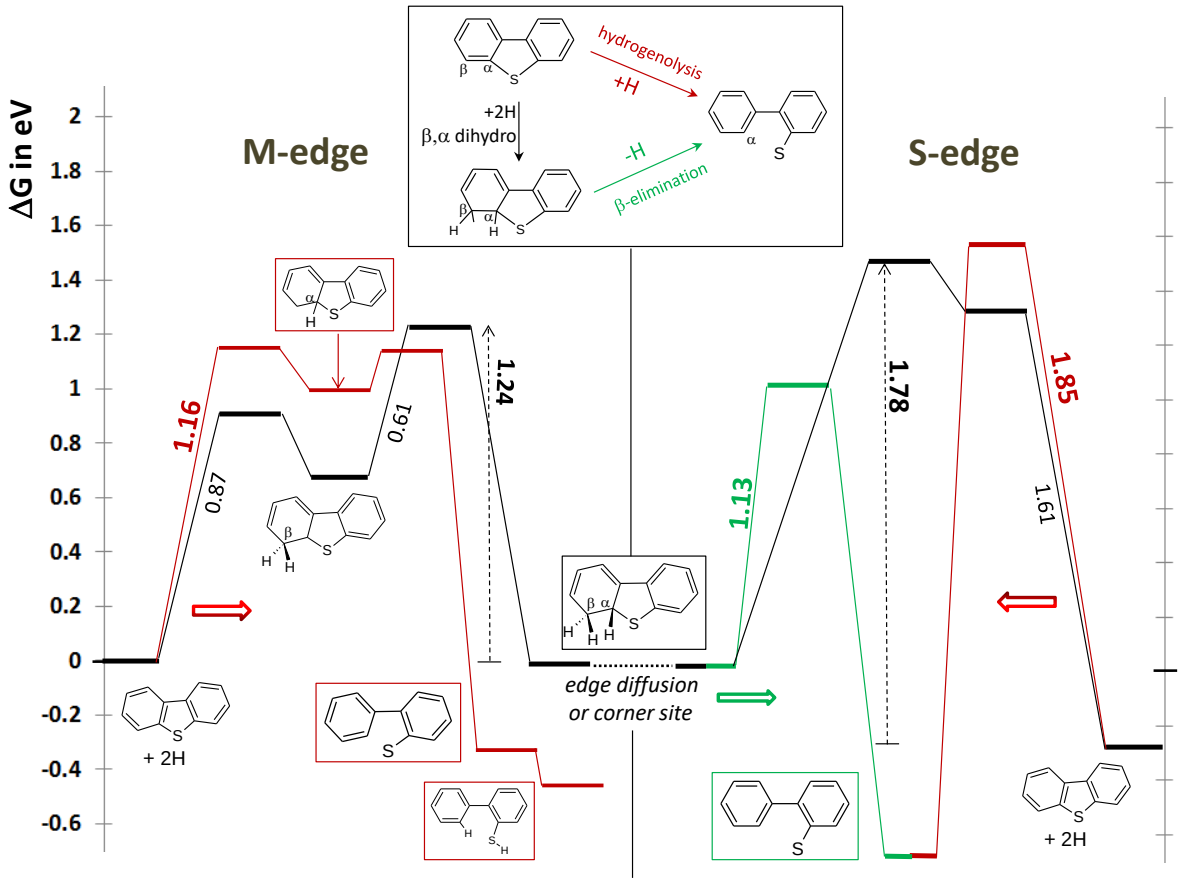

Fig. 11. Summary of the most relevant free energy profiles for the first C-S bond scission of DBT involving the hydrogenolysis pathway (red) and β,α-dihydrogenation steps (black) on the partially Co-promoted M-edge (left panel) and promoted S-edge (right panel). The β–elimination (green) occurs on the S-edge after β,α-dihydrogenation either on the S-edge or on M-edge assuming diffusion or corner site. The energy level of the S-edge is corrected by the energy required for S-diffusion to be consistent with the energy level of M-edge.

The α,β–DHDBT dehydrogenated intermediate is preferentially formed when the first monohydrogenation occurs on the C_β atom of DBT followed by the second monohydrogenation on the C_α atom (through Mo-SH). This result is consistent with the earlier proposal by Mijoin et al. [24]. In this case, it is important to notice that the DHDBT formation involves a competitive activation free energy (+1.24 eV), revealing that this pathway cannot be excluded with respect to the hydrogenolysis mechanism on the same edge site.

On the M-edge with paired Co-Co-Mo-Mo sites, we identified a unique mechanism where the first monohydrogenation occurs on the C_β atom of DBT and the second one leads to the α,β–DHDBT intermediate. The activation energies are slightly higher than those obtained on the M-edge with alternated Co-Mo-Co-Mo sites, which may be explained by the fact that the hydrogenating site is a Co-H species instead of a Mo-SH.

For the two S-edge models considered here, the most favorable pathway involves the formation of the α,β–DHDBT intermediate through the preliminary hydrogenation of the C_β atom of DBT. The overall activation energies are higher than those found on the M-edge (+1.78 eV for the S-edge involving one S-vacancy site and one S_2 dimer) which indicates that the hydrogenation pathway is kinetically less favored on the S-edge than on the M-edge. The hydrogenolysis pathway is slightly less favored with an activation energy of +1.85 eV which is significantly higher than on the M-edge. Hence, the partially Co-promoted M-edge is more active for both hydrogenolysis and dehydrogenation of DBT.

Interestingly, we showed the possible existence of a β–elimination mechanism involving α,β–DHDBT with simultaneous S-C scission, corresponding to elimination of E2 type as earlier

proposed by Bataille et al. [25]. The corresponding activation free energy of +1.13 eV reveals that this mechanism is strongly competing with the hydrogenolysis pathway calculated on the M-edge sites (present work) or on other sites reported in the literature [35, 37, 38]. For that, the transient local architecture of the active sites must combine one S-vacancy (CUS) together with one neighboring S_2 dimer which is directly involved as active center for the β–H elimination. This architecture results from the diffusion process of S-atom on the edge which involves free energy barriers compatible with the whole HDS mechanism. The S-diffusion is also more favorable than the direct S-removal process. From an experimental point of view, we hope that future progress of operando spectroscopies will help to identify the presence of such transient S_2 species during HDS and their role on the β-elimination pathway.

At this stage, it was not possible to identify a TS for the β–elimination mechanism on the M-edge. Due to the rather complex intrinsic nature of the TS involving several intricated bond cleavage and formation as observed on the S-edge, progress on theoretical approach based on biased ab initio molecular dynamics will help to solve this open question [71]. In the present state, we propose that a possible optimal scenario for the hydrodesulfurization of DBT should actually combine both edges as illustrated in **Fig. 11**. The M-edge initiates the formation of the α,β–DHDBT intermediate at moderate activation energy. Then, DHDBT should diffuse from the M-edge to the S-edge. Although more investigation is required in the future on this event, diffusion seems possible considering the very close energy levels of DHDBT on both edges. Then, β–elimination mechanism with C-S bond scission occurs on the S-edge. Since previous studies [10, 37, 38, 70] suggested the specific role of corner sites, a DHDBT molecule formed on such a corner site could also benefit from a synergy effect between the close vicinity of the two edges. However, such a scenario requires specific design of the active phase where partial

promotion of the M-edge and full promotion of the S-edge are simultaneously present on the CoMoS nano-crystallites. Standard CoMoS catalysts may not provide such an optimal configuration which requires to carefully tune CoMoS morphology, Co/Mo ratio and edge distribution of Co atom during the synthesis or activation steps, as proposed for other HDS reaction [9].

Finally, during the β−elimination mechanism identified here, the specific stereochemistry of the leaving H_β atom distinct from the H_β atom previously added at hydrogenation may explain for one part, the strong decrease of the DDS pathway of 4,6-alkyl substituted DBT compounds where only one H_β atom is available. In addition, we suggest to investigate the impact of akyl substituents on the rotational movement of the phenyl-group at transition states and on the corresponding activation energies identified in the present work, as a function of the edge sites. This would also enable to analyze the origin of the DDS/HYD pathways as a function of the reactant and of the active phase features. In order to better discriminate more clearly between these mechanisms, it would also be welcome to establish a microkinetic model based on the present DFT data.

Acknowledgements

The authors would like to thank T. Bučko (Comenius University in Bratislava) and J. Rey (IFP Energies nouvelles – Ecole Normale Supérieure de Lyon) for fruitful discussions and advice on IRC analysis.

Fundings

The calculations were performed using HPC resources (Jean Zay and Occigen) from GENCI-CINES (Grant A0020806134) and ENER 440 from IFP Energies nouvelles. This work is part of the "RatiOnAl Design for CATalysis" (ROAD4CAT) industrial chair, project IDEXLYON funded by the French National Research Agency (ANR-16-IDEX-0005) and the Commissariat-General for Investment (CGI) within the framework of Investissements d'Avenir program ("Investment for the future").

References

[1] R. Prins, Handbook of Heterogeneous Catalysis, Wiley-VHC Verlagsgesellschaft, Weinheim, 1997.
[2] H. Toulhoat, P. Raybaud, Catalysis by Transition Metal Sulfides. From molecular theory to industrial applications., Technip Edition, Paris (France), 2013.
[3] H. Topsøe, B.S. Clausen, F.E. Massoth, Hydrotreating Catalysis - Science and Technology, Springer-Verlag, Berlin/Heidelberg, 1996.
[4] H. Topsøe, B.S. Clausen, R. Candia, C. Wivel, S. Mørup, J. Catal. 68 (1981) 433.
[5] I. Alstrup, I. Chorkendorff, R. Candia, B.S. Clausen, H. Topsoe, J. Catal. 77 (1982) 397.
[6] B.S. Clausen, H. Topsøe, Hyperfine Interact. 47 (1989) 203.
[7] S.M.A.M. Bouwens, J.A.R. van Veen, D.C. Koningsberger, V.H.J. de Beer, R. Prins, J. Phys. Chem. 95 (1991) 123.
[8] J.V. Lauritsen, M.V. Bollinger, E. Lægsgaard, K.W. Jacobsen, J.K. Nørskov, B.S. Clausen, H. Topsøe, F. Besenbacher, J. Catal. 221 (2004) 510.
[9] B. Baubet, M. Girleanu, A.-S. Gay, A.-L. Taleb, M. Moreaud, F. Wahl, V. Delattre, E. Devers, A. Hugon, O. Ersen, P. Afanasiev, P. Raybaud, ACS Catal. 6 (2016) 1081.
[10] S. Kasztelan, H. Toulhoat, J. Grimblot, J.P. Bonnelle, Appl. Catal. 13 (1984) 127.
[11] H. Schweiger, P. Raybaud, H. Toulhoat, J. Catal. 212 (2002) 33.

[12] L.S. Byskov, J.K. Nørskov, B.S. Clausen, H. Topsøe, J. Catal. 187 (1999) 109.
[13] P. Raybaud, Appl. Catal. A: Gen. 322 (2007) 76.
[14] X.L. Ma, K.Y. Sakanishi, I. Mochida, Ind. Eng. Chem. Res. 33 (1994) 218.
[15] U.T. Turaga, C.S. Song, Catal. Today 86 (2003) 129.
[16] D.D. Whitehurst, T. Isoda, I. Mochida, Advances in Catalysis, Vol 42 42 (1998) 345.
[17] B.C. Gates, H. Topsøe, Polyhedron 16 (1997) 3213.
[18] M. Daage, R.R. Chianelli, J. Catal. 149 (1994) 414.
[19] E.O. Orozco, M. Vrinat, Appl. Catal. A: General 170 (1998) 195.
[20] V. Vanrysselberghe, R. Le Gall, G.F. Froment, Ind. Eng. Chem. Res. 37 (1998) 1235.
[21] M. Egorova, R. Prins, J. Catal. 225 (2004) 417.
[22] G.H. Singhal, R.L. Espino, J.E. Sobel, G.A. Huff, J. Catal. 67 (1981) 457.
[23] V. Lamure-Meille, E. Schulz, M. Lemaire, M. Vrinat, Applied Catalysis A: General 131 (1995) 143.
[24] J. Mijoin, G. Perot, F. Bataille, J.L. Lemberton, M. Breysse, S. Kasztelan, Catal. Lett. 71 (2001) 139.
[25] F. Bataille, J.L. Lemberton, P. Michaud, G. Perot, M. Vrinat, M. Lemaire, E. Schulz, M. Breysse, S. Kasztelan, J. Catal. 191 (2000) 409.
[26] D.H. Broderick, B.C. Gates, AIChE J. 27 (1981) 663.
[27] V. Meille, E. Schulz, M. Lemaire, M. Vrinat, J. Catal. 170 (1997) 29.
[28] M. Egorova, R. Prins, J. Catal. 241 (2006) 162.
[29] A.K. Tuxen, H.G. Füchtbauer, B. Temel, B. Hinnemann, H. Topsøe, K.G. Knudsen, F. Besenbacher, J.V. Lauritsen, J. Catal. 295 (2012) 146.
[30] J.V. Lauritsen, F. Besenbacher, J. Catal. 328 (2015) 49.
[31] S.S. Gronborg, M. Saric, P.G. Moses, J. Rossmeisl, J.V. Lauritsen, J. Catal. 344 (2016) 121.
[32] S. Humbert, G. Izzet, P. Raybaud, J. Catal. 333 (2016) 78.
[33] D.H. Broderick, A.V. Sapre, B.C. Gates, H. Kwart, G.C.A. Schuit, J. Catal. 73 (1982) 45.
[34] S. Cristol, J.F. Paul, E. Payen, D. Bougeard, F. Hutschka, S. Clemendot, J. Catal. 224 (2004) 138.
[35] T. Weber, J.A.R. van Veen, Catal. Today 130 (2008) 170.
[36] J.-F. Paul, S. Cristol, E. Payen, Catal. Today 130 (2008) 139.
[37] M. Saric, J. Rossmeisl, P.G. Moses, J. Catal. 358 (2018) 131.
[38] S.J. Ding, Y.S. Zhou, Q. Wei, S.J. Jiang, W.W. Zhou, Catal. Today 305 (2018) 28.
[39] E. Krebs, B. Silvi, P. Raybaud, Catal. Today 130 (2008) 160.
[40] A.D. Gandubert, E. Krebs, C. Legens, D. Costa, D. Guillaume, P. Raybaud, Catal. Today 130 (2008) 149.
[41] A. Travert, C. Dujardin, F. Maugé, E. Veilly, S. Cristol, J.-F. Paul, E. Payen, J. Phys. Chem. B 110 (2006) 1261.
[42] F. Caron, M. Rivallan, S. Humbert, A. Daudin, S. Bordiga, P. Raybaud, J. Catal. 361 (2018) 62.
[43] P. Hohenberg, W. Kohn, Phys. Rev. B 136 (1964) 864.
[44] W. Kohn, L.J. Sham, Phys. Rev. A 140 (1965) 1133.
[45] G. Kresse, J. Furthmüller, Comput. Mater. Sci. 6 (1996) 15.
[46] G. Kresse, J. Furthmüller, Phys. Rev. B 54 (1996) 11169.
[47] J.P. Perdew, K. Burke, M. Ernzerhof, Phys. Rev. Lett. 77 (1996) 3865.
[48] G. Kresse, D. Joubert, Phys. Rev. B 59 (1999) 1758.
[49] S.N. Steinmann, C. Corminboeuf, J. Chem. Phys. 134 (2011).

[50] S.N. Steinmann, C. Corminboeuf, J. Chem. Theory Comput. 7 (2011) 3567.
[51] M. Saab, P. Raybaud, J. Phys. Chem. C 120 (2016) 10691.
[52] E. Krebs, B. Silvi, A. Daudin, P. Raybaud, J. Catal. 260 (2008) 276.
[53] P. Fleurat-Lessard, Opt'n path software, http://pfleurat.free.fr/ReactionPath.php, in.
[54] G. Henkelman, H. Jonsson, J. Chem. Phys. 113 (2000) 9978.
[55] G. Henkelman, B.P. Uberuaga, H. Jonsson, J. Chem. Phys. 113 (2000) 9901.
[56] G. Henkelman, H. Jónsson, J. Chem. Phys. 111 (1999) 7010.
[57] K. Fukui, The Journal of Physical Chemistry 74 (1970) 4161.
[58] K. Fukui, Acc. Chem. Res. 14 (1981) 363.
[59] B.A. De Moor, M.-F. Reyniers, G.B. Marin, Phys. Chem. Chem. Phys. 11 (2009) 2939.
[60] A. Travert, H. Nakamura, R.A. van Santen, S. Cristol, J.F. Paul, E. Payen, J. Am. Chem. Soc. 124 (2002) 7084.
[61] A.B. Anderson, Z.Y. Alsaigh, W.K. Hall, J. Phys. Chem. 92 (1988) 803.
[62] T. Todorova, R. Prins, T. Weber, J. Catal. 236 (2005) 190.
[63] T. Todorova, R. Prins, T. Weber, J. Catal. 246 (2007) 109.
[64] C. Dupont, R. Lemeur, A. Daudin, P. Raybaud, J. Catal. 279 (2011) 276.
[65] S. Kozuch, S. Shaik, Acc. Chem. Res. 44 (2011) 101.
[66] Y. Sun, R. Prins, J. Catal. 267 (2009) 193.
[67] Y. Okamoto, M. Kawano, T. Kawabata, T. Kubota, I. Hiromitsu, J. Phys. Chem. B 109 (2005) 288.
[68] P. Afanasiev, J. Catal. 269 (2010) 269.
[69] M.V. Bollinger, J.V. Lauritsen, K.W. Jacobsen, J.K. Norskov, S. Helveg, F. Besenbacher, Phys. Rev. Lett. 87 (2001).
[70] H. Schweiger, P. Raybaud, G. Kresse, H. Toulhoat, J. Catal. 207 (2002) 76.
[71] J. Rey, C. Bignaud, P. Raybaud, T. Bučko, C. Chizallet, Angewandte Chemie International Edition 59 (2020) 18938.